Neuron, Vol. 35, 291–306, July 18, 2002, Copyright ©2002 by Cell Press

Drosophila VAP-33A Directs Bouton Formation at Neuromuscular Junctions in a Dosage-Dependent Manner

Giuseppa Pennetta,[1,2] Peter Robin Hiesinger,[1,2] Ruth Fabian-Fine,[5] Ian A. Meinertzhagen,[5] and Hugo J. Bellen[1,2,3,4,6]
[1]Howard Hughes Medical Institute
[2]Department of Human and Molecular Genetics
[3]Division of Neuroscience
[4]Program in Developmental Biology
Baylor College of Medicine
One Baylor Plaza
Houston, Texas 77030
[5]Neuroscience Institute
Life Sciences Centre
Dalhousie University
Halifax, Nova Scotia
Canada B3H 4J1

Summary

***Aplysia* VAP-33 (VAMP-associated protein) has been previously proposed to be involved in the control of neurotransmitter release. Here, we show that a *Drosophila* homolog of VAP-33, DVAP-33A, is localized to neuromuscular junctions. Loss of *DVAP-33A* causes a severe decrease in the number of boutons and a corresponding increase in bouton size. Conversely, presynaptic overexpression of DVAP-33A induces an increase in the number of boutons and a decrease in their size. Gain-of-function experiments show that the presynaptic dose of DVAP-33A tightly modulates the number of synaptic boutons. Our data also indicate that the presynaptic microtubule architecture is severely compromised in *DVAP-33A* mutants. We propose that a DVAP-33A-mediated interaction between microtubules and presynaptic membrane plays a pivotal role during bouton budding.**

Introduction

Our movements are controlled by the output of neuronal circuits that transmit information to muscles via a specialized type of synapse, the neuromuscular junction (NMJ). Various changes can alter these synaptic connections and the strength of their transmission, revealing a significant capacity for plasticity (Budnik and Gramates, 1999; Sanes and Lichtman, 1999). Similar changes may underlie the cellular basis of learning and memory at central synapses (Engert and Bonhoeffer, 1999; Maletic-Savatic et al., 1999; Toni et al., 1999). Compared with central synapses, however, the advantages of NMJs are their relative size, organizational simplicity, and accessibility to experimental manipulation. These advantages are supplemented in the fruit fly by sophisticated genetic tools and the availability of numerous NMJ markers (Bellen and Budnik, 2000).

After the formation of the first contacts between motor neurons and muscles, at the end of embryonic development, *Drosophila* NMJs undergo a dynamic expansion throughout the larval period. As the larva grows from first to third instar, the surface of the postsynaptic muscle increases 100-fold, whereas the presynaptic terminal undergoes a 10-fold increase in number of boutons and active zones (Schuster et al., 1996a). This growth occurs both by adding new boutons and by increasing the number of synaptic branches. New boutons form, at least in part, by asymmetric division of preexisting ones in a process resembling budding in yeast (Zito et al., 1999). The extensive and well-defined features of growth during the transition from first to third instar larvae make the *Drosophila* NMJ a sensitive system to assess the role of specific proteins during this growth phase.

The development of NMJs in fruit flies is regulated by activity-dependent processes as first demonstrated in mutants with increased neuronal activity or cAMP. In K^+ channel mutants, such as *ether a go-go* (*eag*) and *Shaker* (*Sh*), increased electrical activity is paralleled by an increased number of varicosities and branches at NMJs (Budnik et al., 1990; Zhong et al., 1992). A similar phenotype is also associated with a 50% loss in Fasciclin II (FasII), the *Drosophila* homolog of the cell adhesion molecule apCAM (Schuster et al., 1996b). Mutations with increased cAMP and enhanced synaptic activity have decreased FasII levels along with increased sprouting, consistent with the idea that synaptic growth is controlled by electrical activity (Davis et al., 1996; Schuster et al., 1996a, 1996b).

Recently, phenotypic characterization of mutations in two other *Drosophila* genes, *futsch* and *still life*, revealed that cytoskeletal components may also play an important role in synapse modeling. *futsch* encodes a microtubule-associated protein (MAP) recognized by mAb22C10 (Hummel et al., 2000). The effects of its loss suggest that the microtubule cytoskeleton may modulate synaptic growth and sprouting of boutons (Roos et al., 2000). *still life,* on the other hand, encodes a guanine nucleotide exchange factor for the Rho family of small G proteins (Sone et al., 1997). The protein is present at NMJs and mutations in *still life* cause a shortening of synaptic branches and a reduction in number of boutons. It is thought that *still life* controls the shape of the synaptic terminal by controlling the organization of its actin cytoskeleton (Sone et al., 1997). These studies therefore suggest that both actin and microtubules may be required for specific aspects of bouton formation and synaptic maturation.

Our initial interest in VAP-33 (VAMP-associated protein of 33 kDa) was prompted by the proposal that it functions as a positive regulator of neurotransmitter release (Skehel et al., 1995). A range of subcellular localizations and functions has subsequently been suggested for VAP-33 homologs. In humans, VAP-33 (hVAP-33) binds occludin, a protein located at the tight junctions of epithelial cells. Overexpression of hVAP-33 induces occludin to relocalize along the lateral edge of the plasma membrane (Lapierre et al., 1999). In the rat, VAP-33 is located at the endoplasmic reticulum (ER) and pre-Golgi intermediates and it is proposed to act early in the

[6]Correspondence: hbellen@bcm.tmc.edu

secretory pathway, possibly within the Golgi apparatus itself or between the Golgi apparatus and the ER (Soussan et al., 1999). In the mouse, VAP-33 is localized at the ER as well as in association with microtubules (Skehel et al., 2000). In yeast, the VAP-33 homolog (Scs2) is an integral membrane protein located at the ER (Kagiwada et al., 1998), where it functions to suppress inositol auxotrophy (Nikawa et al., 1995). Finally, plant homologs of VAP-33 have been identified that localize to the plasma membrane and are induced by osmotic stress (Galaud et al., 1997; Laurent et al., 2000). These findings do not provide a coherent picture of the function of this protein family. One obvious interpretation, however, is that different isoforms play different roles in different cells.

Here, we report the identification and characterization of a homolog of VAP-33 in *Drosophila* (DVAP-33A). We show that DVAP-33A is expressed at the larval neuromuscular junctions, where it regulates synaptic bouton budding in a dosage-dependent manner. Our data suggest that DVAP-33A regulates the division of boutons at the synaptic terminals by stabilizing and directing the microtubule cytoskeleton during budding.

Results

Identification of *Drosophila* VAP-33 Homolog and Mutational Analysis of *DVAP-33A*

Given that the VAP-33 protein in *Aplysia* has been proposed to be a regulator of neurotransmitter release (Skehel et al., 1995), we screened for *Drosophila* homologs of VAP-33 (Lloyd et al., 2000). Our search revealed three structural homologs displaying 39% (*farinelli*), 18% (*DVAP-33B*), and 40% (*DVAP-33A*) identity to *Aplysia* VAP-33, respectively. Of these, *farinelli* is specifically expressed in testes and required for male fertility (Accession Number AF280798). As the homology of DVAP-33B with VAP-33 is rather low, we decided to focus on *DVAP-33A*. In situ hybridization to polytene chromosomes showed that *DVAP-33A* maps to 3F5-6 on the X chromosome. The locus comprises seven exons (Figure 1A). Developmental Northern blot analysis identified four transcripts that are expressed at all developmental stages (data not shown). We obtained four cDNAs and sequenced the longest. This cDNA contains an ORF encoding a putative protein of 269 amino acids. We raised polyclonal antibodies, and Western blot analysis from wild-type (CS) second instar larvae revealed a single band of 35 kDa (Figure 1B), in agreement with the estimated molecular weight.

To create mutations in *DVAP-33A*, we searched for P element insertions in 3F and identified $P\{ry^{+t7.2}=lArB\}47$ (Figure 1A; Bellen et al., 1989). This P element insertion maps about 600 bp upstream of the presumptive AUG. Homozygous $P\{ry^{+t7.2}=lArB\}47$ flies are viable and fertile, and Western blot analysis showed that their DVAP-33A protein levels do not differ from those of wild-type (data not shown). To create novel mutations, we generated imprecise ($DVAP\text{-}33A^{\Delta 20}$, $DVAP\text{-}33A^{\Delta 448}$, and $DVAP\text{-}33A^{\Delta 166}$) excisions of $P\{ry^{+t7.2}=lArB\}47$ (Figure 1D). $DVAP\text{-}33A^{\Delta 448}$ and $DVAP\text{-}33A^{\Delta 20}$ remove, respectively, 1.5 kb and 2.0 kb of genomic region surrounding the original P element insertion. Both mutations are null alleles since no wild-type protein was detectable by Western blot analysis (Figure 1B). Hemizygous mutant males exhibit severe locomotion defects and die as second- or early third instar larvae. The lethality associated with both alleles was rescued by ubiquitous expression of DVAP-33A using a *P{hs-DVAP-33A}* transgene and repeated mild heat shock treatments. Larvae with a precise excision of the original P element insertion, $DVAP\text{-}33A^{\Delta 466}$, produce a wild-type amount of protein, and do not exhibit obvious phenotypes (Figure 1D). We also isolated a hypomorph allele, $DVAP\text{-}33A^{\Delta 166}$, that encodes a truncated protein of about 20 kDa.

Homologs of *VAP-33* have been identified in a variety of species, suggesting a conserved functional role for *DVAP-33A*. The overall structure of the protein is similar in all species and exhibits three domains (Figure 1C). The 100 aa N-terminal domain (Figure 1C) exhibits significant homology (25% identity, 45% similarity) to the nematode major sperm protein (MSP). This domain contains a 16 aa domain (Figure 1C) of unknown function that is identical in most VAP-33 homologs. The central domain of the protein contains a 44 aa coiled-coil domain as predicted by the COILS algorithm (90% probability). Finally, a C-terminal hydrophobic region (Figure 1C) probably anchors the protein into the membrane. The overall homology to other VAP-33 proteins is shown in Figure 1E.

DVAP-33A Is Localized Pre- and Postsynaptically at Neuromuscular Junctions

In *Drosophila*, DVAP-33A is widely expressed from the earliest stages of embryonic development onward. The protein is mostly associated with cellular membranes, and double staining with anti-DVAP-33A and anti-Discs-Large (DLG) shows that the two proteins colocalize in most or all cells at cellular blastoderm, early gastrulation, and in third instar larvae (data not shown). DVAP-33A is membrane associated but some of the protein is cytoplasmic.

At the third instar larval NMJ (Figure 2), DVAP-33A is localized to glutamatergic synapses of the body wall muscles fibers. To examine its subcellular localization, we double-labeled synapses with anti-DVAP-33A (red) and either a pre- or a postsynaptic marker (green). As shown in Figures 2A–2C, DVAP-33A overlaps only partially with the membrane-associated antigen and presynaptic marker, anti-horseradish peroxidase (anti-HRP; Jan and Jan, 1982). Double labeling of the same synapses with anti-DVAP-33A and anti-DLG, which marks both pre- and postsynaptic sites (Lahey et al., 1994), shows that both proteins colocalize (Figures 2D–2F). DVAP-33A exhibits the same localization pattern at the synaptic boutons of wild-type second instar larvae (data not shown). These data suggest that DVAP-33A is localized to both the pre- and postsynaptic compartments of the NMJ.

To define the subsynaptic localization of DVAP-33A more precisely, we analyzed three-dimensional (3D) visualizations of high-resolution confocal data. These allowed us not only to analyze the 3D structure, but also to remove portions to show protein localization inside the bouton. Our analysis revealed that DVAP-33A and DLG not only colocalize, but that both are specifically excluded from particular areas of the bouton's membrane (Figures 2G–2I). These observations confirm those

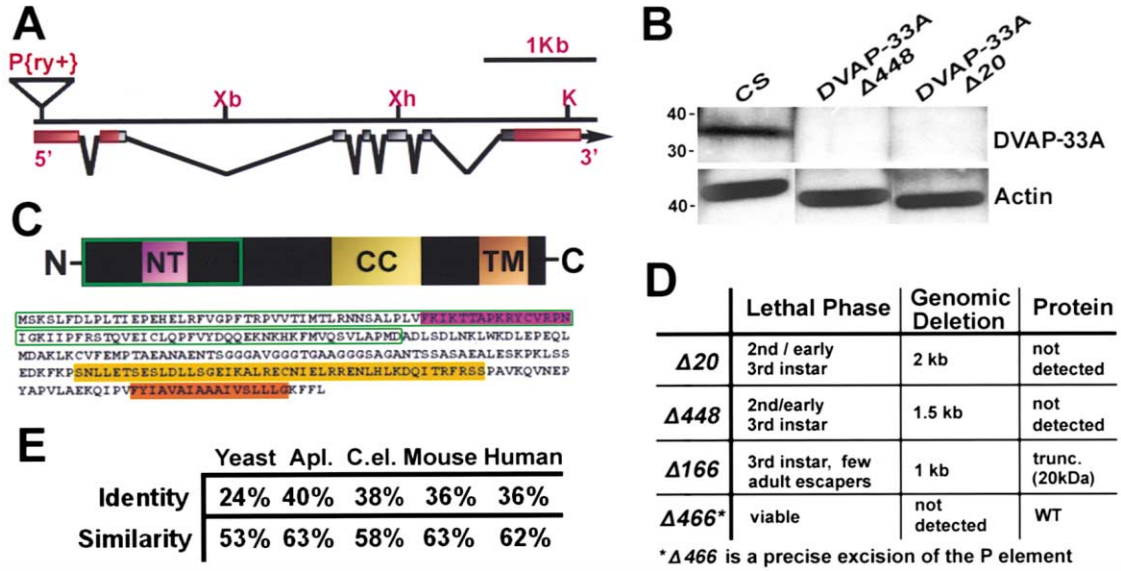

	Lethal Phase	Genomic Deletion	Protein
Δ20	2nd / early 3rd instar	2 kb	not detected
Δ448	2nd/early 3rd instar	1.5 kb	not detected
Δ166	3rd instar, few adult escapers	1 kb	trunc. (20kDa)
*Δ466**	viable	not detected	WT

**Δ466* is a precise excision of the P element

Figure 1. Genomic Structure, Protein Sequence, and Mutational Analysis of DVAP-33A

(A) The *DVAP-33A* gene consists of seven exons: the 5′ and 3′ UTR are boxed in red, the ORF in black. Xb (XbaI); Xh (XhoI); K (KpnI). (B) Western blot of Canton S (CS), *DVAP-33A*$^{\Delta 448}$, and *DVAP-33A*$^{\Delta 20}$ second instar larvae using anti-DVAP-33A antibody. A single band of about 35 kDa is detected in CS larvae while no band is detected in hemizygous mutant larvae. As loading control, we used anti-actin antibody. (C) Deduced amino acid sequence and structural domains of DVAP-33A. The boxed area (green) corresponds to a domain of significant homology to the nematode major sperm protein (MSP). A short N-terminal (NT) region (purple) of unknown function is identical in all VAP-33 homologs. A coil-coiled domain (CC) (yellow) and a transmembrane domain (TM) (orange) are also present. (D) Characterization of three mutant alleles of *DVAP-33A*, *Δ20* (*DVAP-33A*$^{\Delta 20}$), *Δ448* (*DVAP-33A*$^{\Delta 448}$), and *Δ166* (*DVAP-33A*$^{\Delta 166}$). No protein is detected in *Δ20* and *Δ448,* while a truncated protein of about 20 kDa is present in *Δ166* mutants. (E) Degree of identity and similarity between DVAP-33A and homologs in yeast, *Aplysia* (Apl.), *C. elegans*, mouse, and human.

previously reported for DLG by Sone et al. (2000), showing that DLG localizes to periactive zones, regions surrounding active zones. We therefore also double-immunolabeled boutons with a marker specific for active zones, anti-DPAK (Sone et al., 2000) and DVAP-33A. DVAP-33A labeling is mostly complementary to that of DPAK (Figures 2K–2O), indicating that DVAP-33A is enriched at periactive zones.

DVAP-33A and DLG Localize Asymmetrically at the Synapse during Bouton Budding

DLG has recently been shown to have a dynamic subcellular distribution which is implicated in polarization of both neuroblast (Ohshiro et al., 2000; Peng et al., 2000) and epithelial cells (Bilder et al., 2000). Since our high-resolution analysis of DVAP-33A immunoreactivity revealed a localization pattern similar and possibly identical to that of DLG, we focused on the protein distribution during bouton formation, i.e., at sites of morphological change. Boutons at the NMJ continuously bud from previous boutons to enlarge their synaptic contact sites with muscles during larval growth (Zito et al., 1999). If DVAP-33A or DLG are involved in bouton polarization and budding, subsynaptic localization of these proteins may differ prior to and during bouton formation. A strong DVAP-33A enrichment is observed at particular sites of the bouton membrane (Figures 3A and 3B). In synaptic profiles showing an emerging bouton, immunoreactivity of the protein increases in areas immediately surrounding the bud (Figure 3B, arrowheads). At newly formed boutons, immunoreactivity is increased at their base or neck (Figures 3A and 3B, arrows). We also found that newly formed boutons often include active zones identified by anti-DPAK immunolabeling (Figure 3B, between arrowheads). While dynamic localization of a given protein can only be shown by live visualization, the irregular distribution of DVAP-33A at putative sites of bouton formation suggests that this protein may undergo active relocalization.

To test whether increased DVAP-33A expression at particular sites of the bouton membrane during synaptic growth is an unspecific phenomenon observed for other membrane markers, we performed a high-resolution analysis of budding boutons double-labeled with anti-DVAP-33A and anti-HRP. This revealed that anti-HRP immunoreactivity is more uniformly distributed than DVAP-33A immunoreactivity (Figures 3C–3E). Interestingly, double labeling for DLG and DVAP-33A shows that both proteins are enriched at the same sites (Figures 3F–3H). In summary, immunoreactivity to DVAP-33A increases at sites where budding is likely to occur, and at putative budding profiles the protein seems to be enriched around the tip of the emerging bouton and at the neck of the bud.

DVAP-33A Is Not Only a Membrane—But Also a Microtubule-Associated Protein

To define the characteristic pattern of DVAP-33A localization at higher resolution, we investigated DVAP-33A expression using immuno-electron microscopy. In serial sections through budding boutons (Figures 4A–4D), silver-enhanced gold particles are located along the plas-

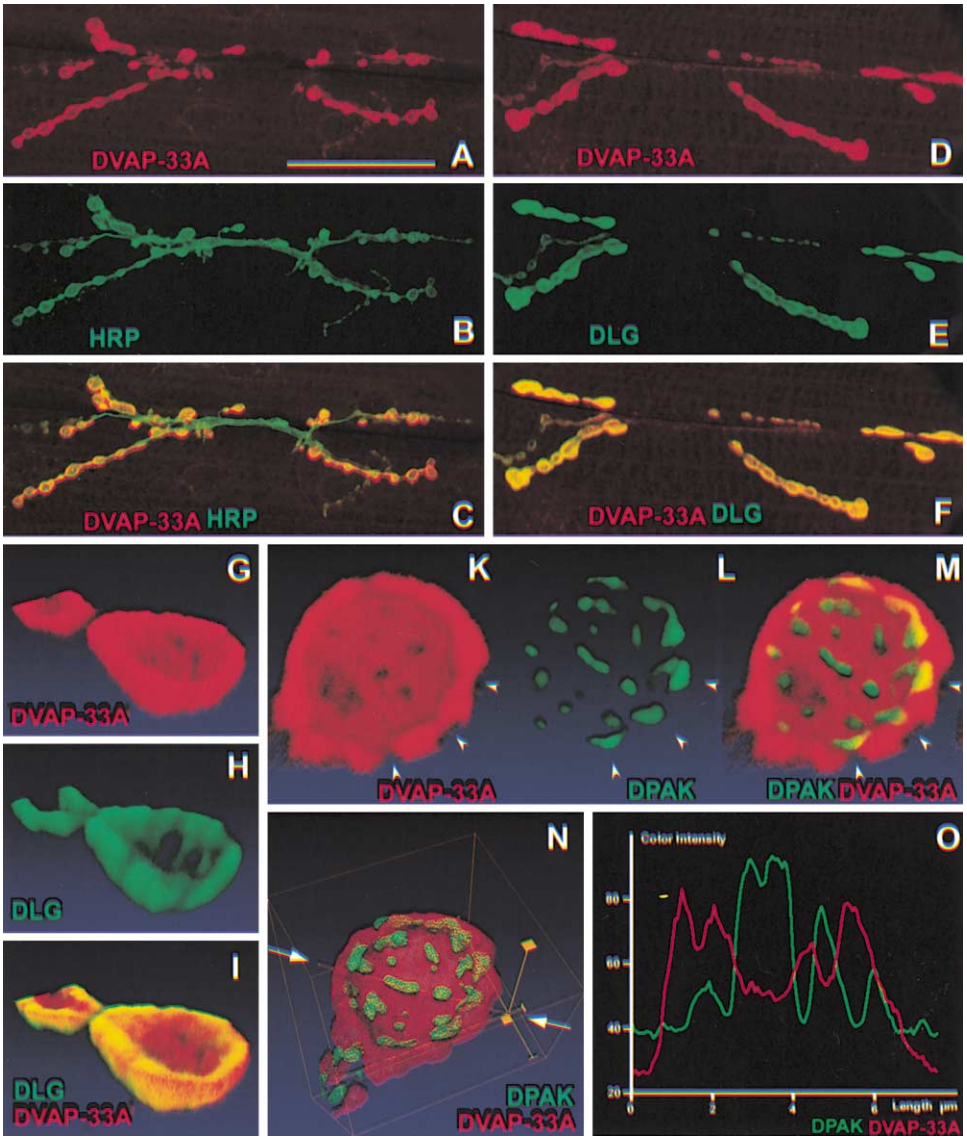

Figure 2. DVAP-33A Is Localized Pre- and Postsynaptically at Neuromuscular Junctions

(A–C) Double-labeled NMJs of muscles 6/7 showing partial overlap of DVAP-33A and HRP immnoreactivity. (D–F) Double-labeled NMJs of muscles 6/7 show complete overlap between DVAP-33A and DLG immnoreactivities. (G–N) DVAP-33A immunoreactivity marks the periactive zones. (G–I) Sectioned volume renderings of double-labeled boutons show patchy labeling for DVAP-33A and DLG at high resolution. (K–O) Double labeling with anti-DPAK and anti-DVAP-33A. DPAK is a marker for active zones. The complementary localization patterns of DPAK and DVAP-33A at high resolution, shown graphically in (O) along the transect in (N) (arrows), suggests that DVAP-33A specifically labels periactive zones, as does DLG. Scale bar for (A)–(F) in (A): 50 μm. Volume shown in (G)–(H): 6 × 7 × 3 μm; (K–O): 8 × 8 × 3 μm

malemma close to the budding site, resembling the pattern of DVAP-33A labeling seen at the light microscopic level (Figures 3A and 3B). Systematic analysis of serial sections revealed, however, that labeling along the neuronal membrane is not restricted to regions where neurons give rise to new boutons, but is also found in other regions (Figures 4E–4G).

In addition to labeling specific regions at the membrane, immunogold particles also extend from the membrane toward the bouton's interior (Figure 4G and inset) as well as in regions separated from the cell membrane, in the interior of the boutons (Figure 4F). Since VAP-33 in mice has previously been shown to be associated with microtubules (Skehel et al., 2000), we tested whether the *Drosophila* protein is also associated with microtubules. Even though microtubules are present inside synaptic boutons (Atwood et al., 1993), the great abundance of 30–50 nm synaptic vesicles made the cross-sectioned profiles of microtubules, 24 nm in diameter, difficult to recognize in tissue fixed and processed for immunolabeling. We therefore examined immunolabeling in photoreceptor axons in ommatidial bundles and in axons of lamina cells, where profiles of microtubules are more easily recognized (Figures 4H and 4I). Careful investigation confirmed that immunolabeling inside the axon profiles is often associated with membranes. Immunoreactivity is also found between vesicular structures (v in Figures 4E and 4F) and cross-sectioned profiles resem-

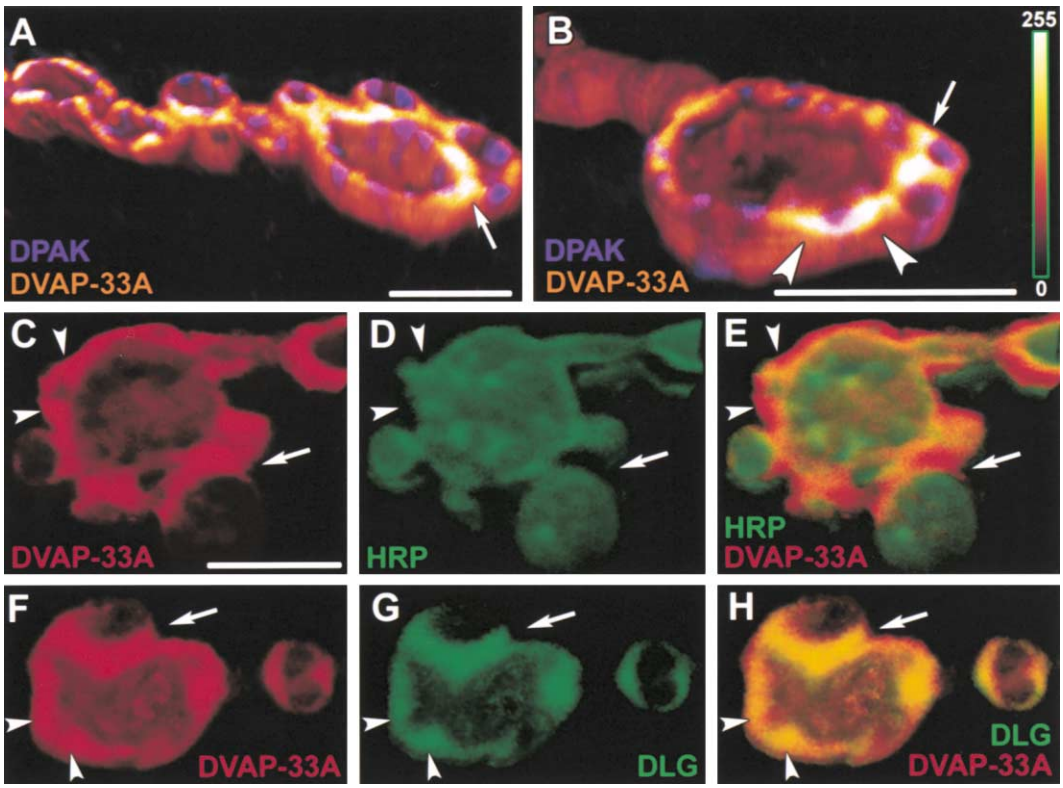

Figure 3. DVAP-33A Is Enriched at Budding Sites

Sectioned volume renderings of double-labeled boutons. (A–B) DVAP-33A and DPAK. DVAP-33A immunoreactivity is shown in a contrast-enhancing color map (right in [B]) in order to correlate overall bouton structure (brown to orange) with places of intense immunoreactivity (yellow to white). DVAP-33A expression is strongly enriched at budding sites, between arrowheads in (B), and remains increased at the base of developing buds (arrows). (C–E) DVAP-33A and HRP. Whereas DVAP-33A shows typical domains of concentration (arrows; newly forming bud between arrowheads), HRP immunoreactivity is more evenly distributed. (F–H) DVAP-33A and DLG. Overlapping domains of concentrated immunoreactivity occur at newly forming buds (arrows) and at emerging buds (between arrowheads). Scale bars: 5 μm. Scale bars for (C)–(H) in (C).

bling microtubules (Figure 4F, arrowheads). Labeled vesicles are usually irregular in shape, with a long axis of approximately 100–150 nm, and occur mainly at the periphery of synaptic sites (Figure 4F). These observations suggest that the labeled vesicular structures are not synaptic vesicles containing neurotransmitter but may instead represent fragments of the endoplasmic reticulum, or Golgi-derived transport vesicles. In conclusion, our ultrastructural analysis suggests that DVAP-33A is associated with both intracellular vesicular structures and plasma membrane, consistent with its primary structure predicting a transmembrane domain at the C terminus. In addition to its association with cell membranes, DVAP-33A also associates with microtubules, often at the sites where vesicles are close to microtubules.

DVAP-33A Associates with Microtubules In Vitro

Since the immuno-electron microscopy revealed a close association between DVAP-33A and bundles of microtubules and since the mouse homolog of DVAP-33A has also been shown to be associated with microtubules (Skehel et al., 2000), we have attempted to determine if DVAP-33A and tubulin cosediment as a complex in vitro (Goode and Feinstein, 1994). We therefore assessed the ability of microtubules to pull down DVAP-33A (Figure 5). Supernatant from adult head extracts was incubated with in vitro polymerized microtubules. A substantial fraction of DVAP-33A cosedimented with microtubules in the pellet fraction in the presence of taxol-stabilized bovine microtubules. In the absence of microtubules, DVAP-33A is found in the supernatant but not in the pellet (Figure 5C). To exclude the possibility that the cosedimentation of DVAP-33A with tubulin is due to an effect of unspecific trapping of the protein by the polymerized microtubules, we performed several controls. Bovine serum albumin (BSA) alone, and an excess of BSA exogenously added to the head extracts, is not pulled down by the addition of the in vitro polymerized bovine microtubules (Figure 5A). The presynaptic protein cysteine string protein (CSP) shows little cosedimentation with microtubules (Figure 5B) when compared with DVAP-33A (Figure 5C). Most of the CSP protein stays in the supernatant (Figure 5B). Hence, DVAP-33A is able to associate with microtubules.

Loss of DVAP-33A Causes Fewer but Larger Boutons at NMJs

DVAP-33A is located at periactive zones, a synaptic region where many molecules controlling synaptic

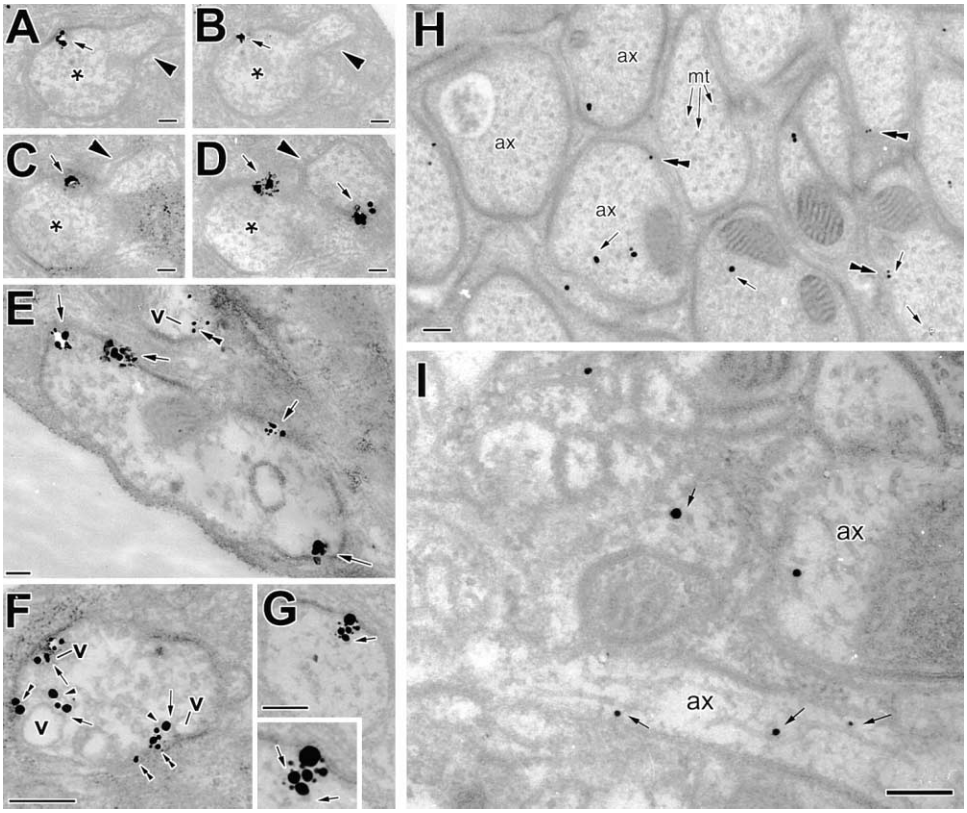

Figure 4. Immunogold Labeling Reveals Membrane and Microtubular Association of DVAP-33A

(A–G) Neuromuscular junctions. (A–D) Cross-sections from a series through a neuronal profile (*asterisk*), from which a second profile emerges (*arrowheads*). Silver-enhanced gold particles are located along the cell membrane close to the budding site (*arrows*). (E) VAP-33-immunolabeling at vesicle-containing neuronal profiles is mainly located close to the cell membrane (*arrows*) and at vesicular structures in the cytoplasm (*double arrowheads*). (F–G) Immunolabeling is found associated with microtubules (*arrows* in [G]) and in (F) at the points of contact (*arrows*) between a vesicle (v) and microtubules (*arrowheads*). *Double arrowheads* in (F) show that most protein is associated with the cell membrane. (H–I) Photoreceptor and optic lobe axons. Immunolabeling in photoreceptor axon profiles (*ax*), including R1–R6, in ommatidial bundles (H), and in neuronal profiles in the lamina (I), demonstrating the microtubular association of particles (*arrows*); *double arrowhead*: labeling close to the plasmalemma; *mt*: microtubules. Scale bars: 200 nm.

growth are clustered (Sone et al., 2000). This subcellular distribution suggest that DVAP-33A could play a role in synaptic development. We therefore examined the morphology of NMJs from second instar larvae *DVAP-33A$^{\Delta 48}$* and *DVAP-33A$^{\Delta 20}$*. These mutants die as second instar/early third instar larvae. We counted the number of larvae boutons on muscles 12 and 13 of abdominal segment 3 and found that the total number of boutons was approximately 50% of wild-type and *DVAP-33A$^{\Delta 66}$* (Figures 6A–6C). Moreover, there was no significant difference in muscle surface area between mutant and control larvae. Although we limited our phenotypic analysis to muscles 12 and 13, the defects described here were observed in all NMJs (data not shown).

To study differences in bouton size, we individually reconstructed the surface areas of all boutons above 2 μm in diameter (types I and III) (Gorczyca et al., 1993; Johansen et al., 1989) on muscles 12 and 13 of ten wild-type and ten mutant NMJs. The number of small boutons (surface area 20–60 μm^2) is substantially decreased in mutants compared with controls, whereas there are many more very large boutons (surface area more than 100 μm^2) in mutants (Figures 6B and 6E). Hence, DVAP-33A mutants exhibit many fewer but larger boutons than control larvae (Figure 6E). Interestingly, the average cumulative synaptic surface areas for all boutons of a single muscle do not differ significantly between controls and *DVAP-33A$^{\Delta 48}$* (Figure 6D). These data indicate that loss of DVAP-33A affects bouton formation but not the global growth of synapses.

DVAP-33A Is an Instructive Signal for Synaptic Bouton Size and Number

To analyze further the effect of altering levels of DVAP-33A on synapse morphology, we studied DVAP-33A overexpression in either wild-type or mutant backgrounds using the UAS/GAL4 system (Brand and Perrimon, 1993). A *UAS-DVAP-33A* transgene was driven either by the pan-neural GAL4 driver *P{elav-GAL4}* (Lin and Goodman, 1994) or the motoneuron-specific GAL4 driver *P{Gal4w1}C164* (Torroja et al., 1999). Increased expression levels of DVAP-33A, using *P{elav-GAL4}* in an otherwise wild-type background, cause a clear increase in bouton number, and a decrease in bouton size compared with the control (UAS line without the GAL4 driver). The number of boutons increases from 253 ($\pm$8)

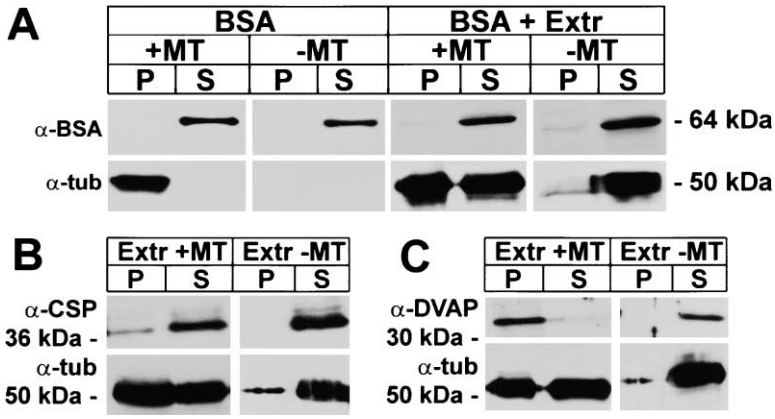

Figure 5. DVAP-33A Cosediments with Microtubules

Microtubules were polymerized in vitro and added to the protein of interest or to head extracts. Binding reactions with (+MT) or without (−MT) microtubules were stratified on a 20% sucrose cushion. The resulting pellets (P) and supernatants (S) were analyzed by SDS-PAGE and Western analysis. (A) Bovine Serum Albumin (BSA) alone and an excess of BSA added to the head extracts (BSA + Extr) were used as negative controls. Head extracts incubated with or without MTs were probed with antibodies specific for the presynaptic protein CSP (B) and for DVAP-33A (C). No major pulldown was observed for CSP, whereas DVAP-33A cosedimented with tubulin in the presence of microtubules but not in their absence. The signal detected by the anti-tubulin antibody in the supernatant (S) in the extracts containing BSA and in the extracts probed for CSP and DVAP-33A is due to the endogenous tubulin.

in control larvae, to 535 (±7) in *P{elav-GAL4}; UAS-DVAP-33A* larvae (Figures 7A and 7B). Similarly, overexpression in *P{Gal4w1}C164*; *UAS-DVAP-33A* larvae causes the bouton number nearly to double (to 459 ± 10, Figure 7C). In both genotypes, the boutons display a remarkable decrease in size that is difficult to quantify because they are so tiny, resembling mere subtle expansions of axons (Figures 7B and 7C). In addition, many synapses exhibit extra branches, although both axonal pathfinding and initial target recognition appear normal.

To correlate the sensitivity of the supernumerary bouton phenotype with expression levels of DVAP-33A, we compared the phenotype of larvae overexpressing DVAP-33A in a wild-type background with that of null mutant larvae (*DVAP-33A*$^{\Delta 448}$) under otherwise identical conditions. By eliminating the endogenous protein, we surmised that the phenotype observed by overexpressing DVAP-33A in wild-type larvae may become attenuated if it were highly sensitive to DVAP-33A levels. The increased number of synaptic boutons at NMJs of such

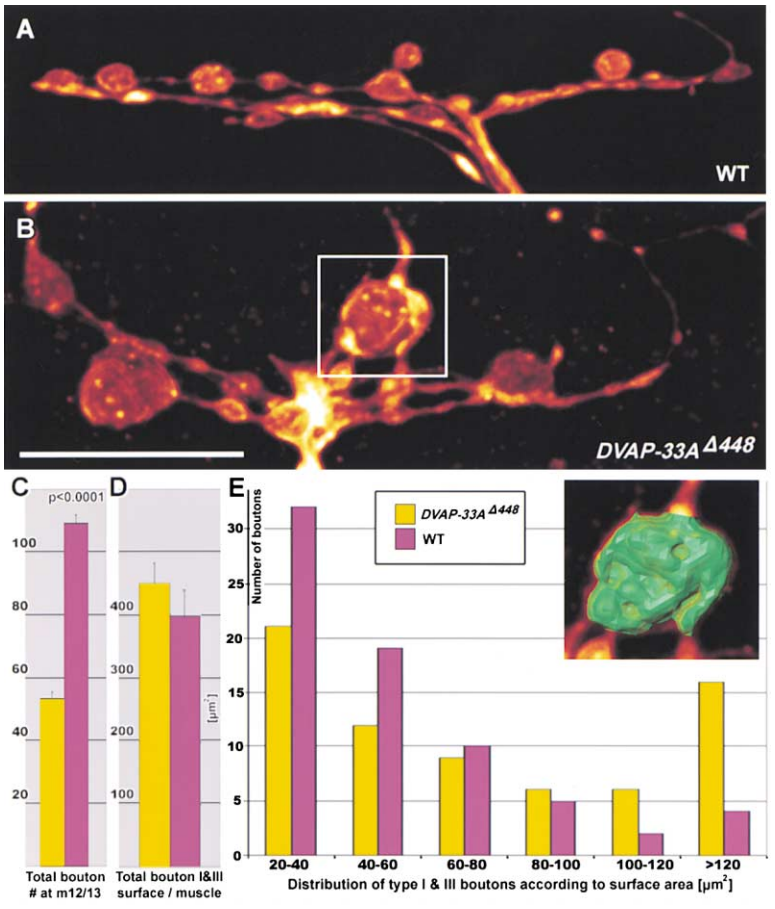

Figure 6. Loss of *DVAP-33A* Causes an Increase in Size and Decrease in Number of Boutons

(A–B) Anti-HRP staining of Canton-S (A) and *DVAP-33A*$^{\Delta 448}$ (B) NMJs at muscle 12. (C–E) Quantification of bouton number and surface areas. (C) Wild-type NMJs at muscles 12 and 13 have approximately twice as many boutons. The total number of boutons at muscles 12 and 13 of abdominal segment 3 of 20 different larvae was counted for both genotypes. (D and E) Quantification of surface areas of boutons at muscles 12 and 13. One hundred and thirty-six boutons larger than 2 μm in diameter (types I & III) were separately surface reconstructed (see inset in [E] which corresponds to the marked bouton in [B] to calculate the surface areas). *DVAP-33A*$^{\Delta 448}$ mutant NMJs display an increased number of large boutons and a decreased number of smaller boutons (E). Despite the redistribution in size observed in the mutant, the calculated total surface area does not significantly differ from that in the wild-type (D). Scale bar for (A) and (B) in (B): 20 μm.

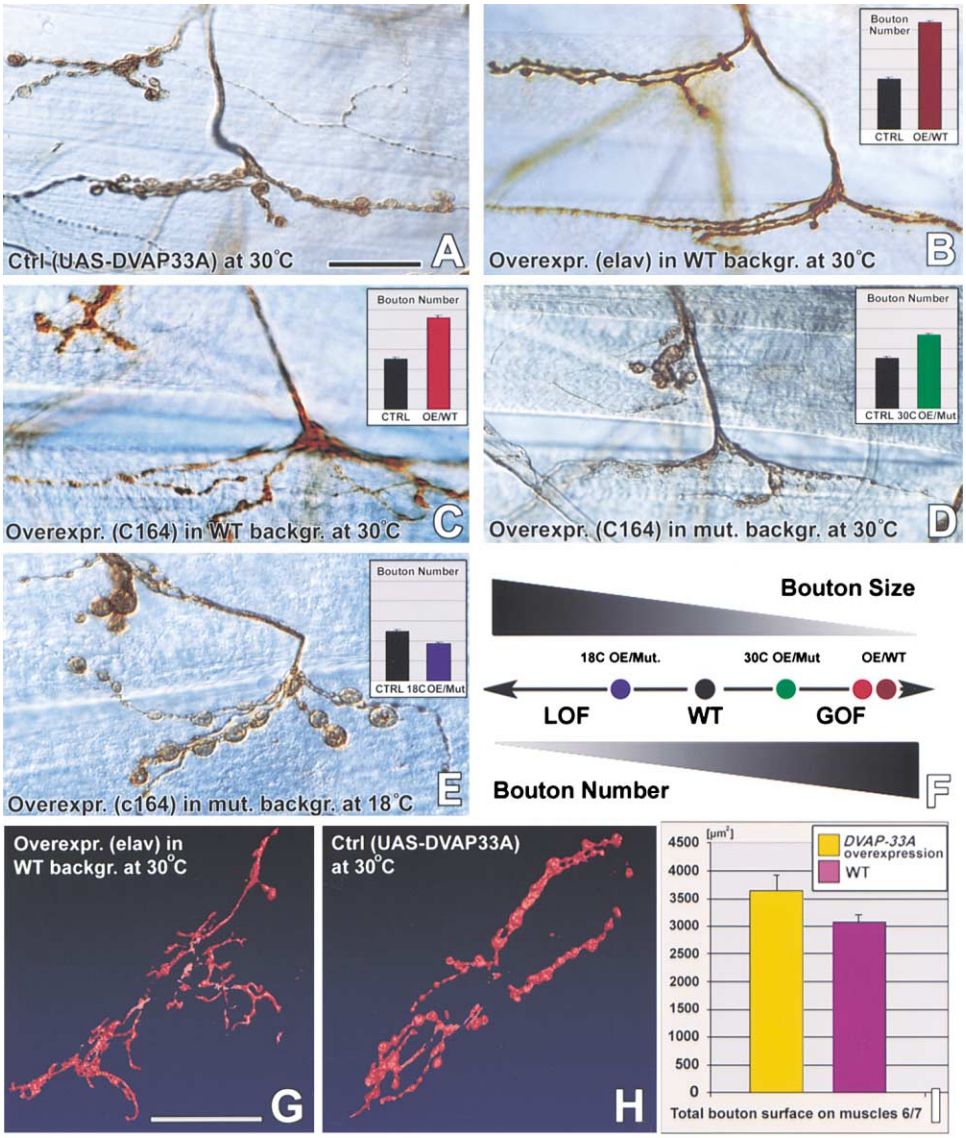

Figure 7. Presynaptic Overexpression of DVAP-33A Induces an Increase in the Number and a Decrease in the Size of Boutons

Third instar larvae of genotypes reported below were stained with anti-HRP, a marker specific for the nervous system. Animals were raised at 18°C or 30°C. Insets show bouton numbers; each subdivision corresponds to 100 boutons and all boutons on muscles 12 and 13 were counted. For every genotype, we counted the total number of boutons on muscles 12 and 13 of the abdominal segment 3 of at least 10 different animals. (A) *UAS-DVAP-33A* NMJs were used as controls. No mutant phenotype at the NMJ was observed in these larvae raised at either 18°C or 30°C. (B) Presynaptic overexpression using *P{elav-GAL4}; UAS-DVAP-33A* or (C) *P{Gal4w1}C164*; *UAS-DVAP-33A*. In both cases, more small boutons were observed. (D) Overexpression of DVAP-33A in *DVAP-33A$^{\Delta 448}$/Y; P{Gal4w1}C164; UAS-DVAP-33A* at 30°C and (E) at 18°C. (F) Diagram summarizing the inverse relationship between bouton size and number as a function of DVAP-33A dosage. NMJs at muscles 6/7 from overexpression lines (G) and controls (H) were stained with the nervous system-specific anti-HRP antibody and the corresponding synapses were surface reconstructed. The quantification of reconstructed surfaces (I) shows a small increase in the total synaptic area in the overexpression but not in the control. The increase was not statistically significant ($p = 0.094$). *UAS-DVAP-33A* larvae raised at 30°C were used as a control. Larvae overexpressing DVAP-33A were: *P{elav-GAL4}; UAS-DVAP-33A* at 30°C. Scale bar in (A) for (A)–(E) 20 μm. Scale bar in (G) for (G) and (H) 50 μm.

larvae is intermediate (367 ± 9) (Figure 7D) and significantly different from those in both control larvae (253 ± 8) and larvae overexpressing DVAP-33A in a wild-type background (459 ± 9) (Figure 7C). In addition, although the sizes of the boutons in *DVAP-33A$^{\Delta 448}$/Y*; *P{Gal4w1}C164*; *UAS-DVAP-33A* larvae are reduced when compared with control boutons (Figure 7A), they are clearly larger than the boutons illustrated in Figures 7B and 7C.

To lower the levels of DVAP-33A, *DVAP-33A$^{\Delta 448}$/Y; P{Gal4w1}C164; UAS-DVAP-33A* animals were kept at 18°C (Figure 7E). At 18°C, the GAL4 protein exhibits much lower activity levels than at 30°C (Greenspan, 1997). Presynaptic expression of DVAP-33A in *DVAP-33A$^{\Delta 448}$/Y; P{Gal4w1}C164; UAS-DVAP-33A* males leads to a reduction of ~50% in the average number of boutons: 367 ± 9 (30°C) versus 188 ± 7 (18°C) (Figures 7D and 7E). The size of the boutons, although not carefully

quantified, is clearly larger at 18°C than at 30°C. Moreover, the number of boutons in *DVAP-33A$^{\Delta 448}$/Y; P{Gal4w1}C164; UAS-DVAP-33A* larvae raised at 18°C is lower than control *UAS-DVAP-33A* raised at the same temperature (Figure 7E, inset). Expression of DVAP-33A in null mutant animals leads to a full rescue of the lethal phenotype, indicating that the lethality is due to the presynaptic loss of DVAP-33A. In summary, the expression level of DVAP-33A plays a pivotal role in synapse development by determining the number and size of boutons at *Drosophila* NMJs. As diagrammed in Figure 7F, there is a direct inverse correlation between bouton size and number. The level of DVAP-33A displays a strong positive correlation with the number of boutons. Despite the dramatic change in bouton number and size, synapses overxpressing DVAP-33A show no significant difference in the total synaptic surface area when compared to controls (Figures 7G–7I). These data indicate that an increase in presynaptic DVAP-33A induces a change in synaptic morphology but not in the total synaptic surface. Taken together, the loss-of-function and gain-of-function experiments show that altering the levels of DVAP-33A is sufficient to determine the number and size of boutons, suggesting that this protein plays an instrumental role in bouton budding.

Mutations in DVAP-33A Affect the Synaptic Microtubule Cytoskeleton

The microtubular association of DVAP-33A and the morphology of the mutant synapse suggest a possible involvement of the cytoskeleton in the DVAP-33A-dependent regulation of bouton size and number. A similar connection was recently shown for Futsch, a microtubule-associated protein recognized by mAb22C10 (Roos et al., 2000; Hummel et al., 2000). Synaptic terminals lacking Futsch protein exhibit a decrease in bouton number and an increase in bouton size. In addition, *futsch* boutons display a disruption in synaptic microtubule organization (Roos et al., 2000), prompting us to investigate whether the synaptic organization of microtubules is also disrupted in *DVAP-33A* mutants.

To visualize the synaptic microtubule cytoskeleton, second- or early third instar larval NMJs were immunolabeled with mAb22C10. In wild-type NMJs, microtubules are organized to form a thread-like structure running through the diameter of the bouton (Roos et al., 2000; Figures 8A–8D). As illustrated for boutons of muscle 12, mAb22C10 immunolabeling is most intense in motoneuron axons and at the branching point, where they contact the surface of target muscles. Labeling fades with increasing distance from the branch points in both wild-type and mutant larval muscles (Figures 8A and 8E). We observed two phenotypic differences at moderately high resolution between wild-type and mutant NMJs. Mutants display increased labeling within the boutons at branching points and exhibit a very different profile of mAb22C10 immunolabeling, with numerous puncta instead of threads (Figures 8A and 8E). Similar observations were made using anti-α-tubulin antibody (data not shown). To characterize the microtubular disruption, we scanned high-resolution 3D confocal datasets of single boutons. A previously tested constrained blind deconvolution algorithm (Hiesinger et al., 2001) was used to remove artificial blur and allow visualization of structures smaller than 500 nm (Figures 8B, 8B′ and 8F, 8F′). Double labeling with anti-DVAP-33A and anti-HRP after separate deconvolution of both channels reveals clear bundles of microtubules inside boutons (Figure 8C). Faint immunoreactivity of fibers at the edge of boutons is not visible without overexposing the immunoreactivity of more central fiber bundles. We therefore made hand-segmented surface reconstructions of the complete microtubular network of these boutons, showing all discernible mAb22C10 immunolabeling regardless of intensity. Three-dimensional views of such reconstructions show a well-organized microtubular network in wild-type boutons with bundles of microtubules running across the boutons and along the membrane. Occasionally, loop-like structures can be observed inside wild-type boutons (Figure 8D). Conversely, the mutant pattern is severely disorganized in about 30% of boutons (Figure 8H, bottom) and totally fragmented in the remaining 70% (Figure 8H, top). Interestingly, in *DVAP-33A$^{\Delta 448}$/Y; P{Gal4w1}C164; UAS-DVAP-33A* NMJs exhibiting an oversprouting phenotype due to presynaptic overexpression of DVAP-33A, the organization of the microtubule cytoskeleton appears significantly more dense and loop-like structures are more easily observed than in wild-type boutons (Figures 8I–8L, arrows). In addition, the microtubule organization appears more sturdy than normal (Figures 8K and 8L). Taken together, these data indicate that the integrity of the cytoskeletal network at the synapse is necessary for bouton division and that DVAP-33A is required for the organization and/or maintenance of the microtubule architecture within the synaptic boutons.

DVAP-33A Is Not Required for the Axonal Transport of Synaptic Components

The subcellular localization of DVAP-33A reveals an association with both microtubules and membranes. This raises the possibility that DVAP-33A functions as a factor controlling the delivery of synaptic components to terminals. To test this possibility, we immunolabeled control and mutant neurons for the synaptic vesicle markers synaptotagmin (SYT) and cysteine string protein (CSP) (data not shown) (Bellen and Budnik, 2000). The localization and level of expression of these proteins are essentially normal in larvae both lacking (Figures 9A–9B) and overexpressing DVAP-33A (Figures 9C–9D). Immunolabeling of larvae deficient for DVAP-33A also revealed that other synaptic components such as Fasciclin II (FasII) and DLG are correctly delivered and localized at DVAP-33A mutant synaptic terminals (Figures 9E–9H). Moreover, mutations in motor proteins or other proteins needed for proper axonal transport have been shown to induce axonal swellings and vesicle/organelle stalling ("organelle jams") along larval segmental nerves (Martin et al., 1999; Gunawardena and Goldstein, 2001). Immunolabeling with synaptic vesicle markers showed that "organelle clogs" are absent in larvae lacking or overexpressing DVAP-33A (data not shown). Finally, in *Drosophila*, mutations removing critical components of the axonal transport machinery share a common neuromuscular phenotype including progressive lethargy and paralysis as well as a typical flipping of the tail during

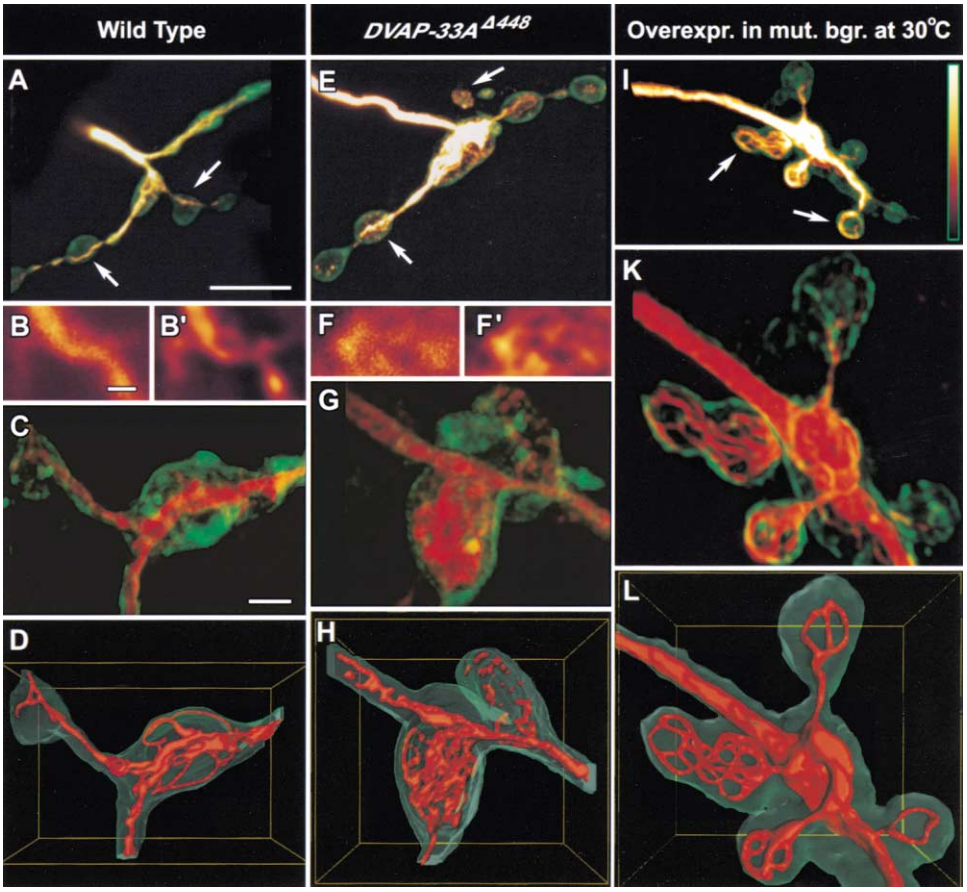

Figure 8. The Three-Dimensional Organization of Microtubules Is Disrupted in *DVAP-33A* Mutant Boutons

(A, E, and I) Visualization of axonal microtubules at axonal branching points using mAb22C10 and the color map depicted in (I). Intense immunoreactivity in the fibers and at the branch point are overexposed to reveal faint staining further away from the branching points. A dimmed green counterstaining with anti-HRP shows the location of boutons. Whereas distinct fibers are clearly recognizable in the wild-type, characteristic punctate labeling within the boutons was observed in mutants (arrows). (B–D, F–H, and K–L) High-resolution 3D deconvolution analysis of microtubular organization inside type I boutons. Wild-type (B, B′, and C), mutant (F, F′, and G), and DVAP33-A overexpression at 30°C (K). (C, G, and K) Maximum intensity projections of deconvolved 3D datasets of mAb22C10 immunoreactivity (red) and anti-HRP immunoreactivity (green). (D, H, and L) Three-dimensional surface reconstructions of the microtubular network inside the boutons irrespective of signal intensity. A disorganized microtubular structure filling the entire bouton as well as isolated punctae is observed in DVAP-33A boutons (G and H) whereas wild-type boutons display distinct microtubular fibers at the center and at the periphery (C and D). Elevated levels of DVAP-33A do not produce visible microtubular disruption (K, L, and data not shown). Scale bar for (A), (E), and (I) in (A): 10 μm; for (B), B′), (F), and (F′) in (B): 500 nm; for (C), (G), and (K) in (C): 2 μm. The volume shown in (D) represents 18 × 13 × 7 μm, the volume in (G) 13 × 13 × 7,5 μm, the volume in (L) 20 × 19 × 8 μm.

larval crawling (Gindhart et al., 1998). Examination of the locomotor ability of larvae lacking DVAP-33A reveals that although they are more sluggish than normal, they exhibit normal crawling behavior. Hence, these data argue against an involvement of DVAP-33A in axonal transport.

Discussion

In this study, we describe the isolation and characterization of *DVAP-33A*. DVAP-33A is a protein that is associated with both membranes and microtubules and is required for the normal organization of the microtubule cytoskeleton in presynaptic terminals. Our data indicate that DVAP-33A acts as an instructive signal to fine-tune synaptic sprouting and bouton budding at NMJs. We propose that it acts by stabilizing the interaction between microtubules and presynaptic membranes during the process of bouton formation.

DVAP-33A: A Major Sperm Protein with a Transmembrane Domain?

VAP proteins share an overall structural organization: they contain a C-terminal transmembrane domain linked by a variable region to an NH2-terminal MSP (major sperm protein) domain. Protein homologs containing an MSP domain fall into two different categories: the MSPs and VAPs.

MSP-like proteins and the structurally related VAP proteins may share a common function. MSPs are small (14 kDa), highly abundant proteins in nematode sperm which form self-assembling filaments at the leading edge of a pseudopod, allowing locomotion of the sperm over short distances (Italiano et al., 1996; Roberts and

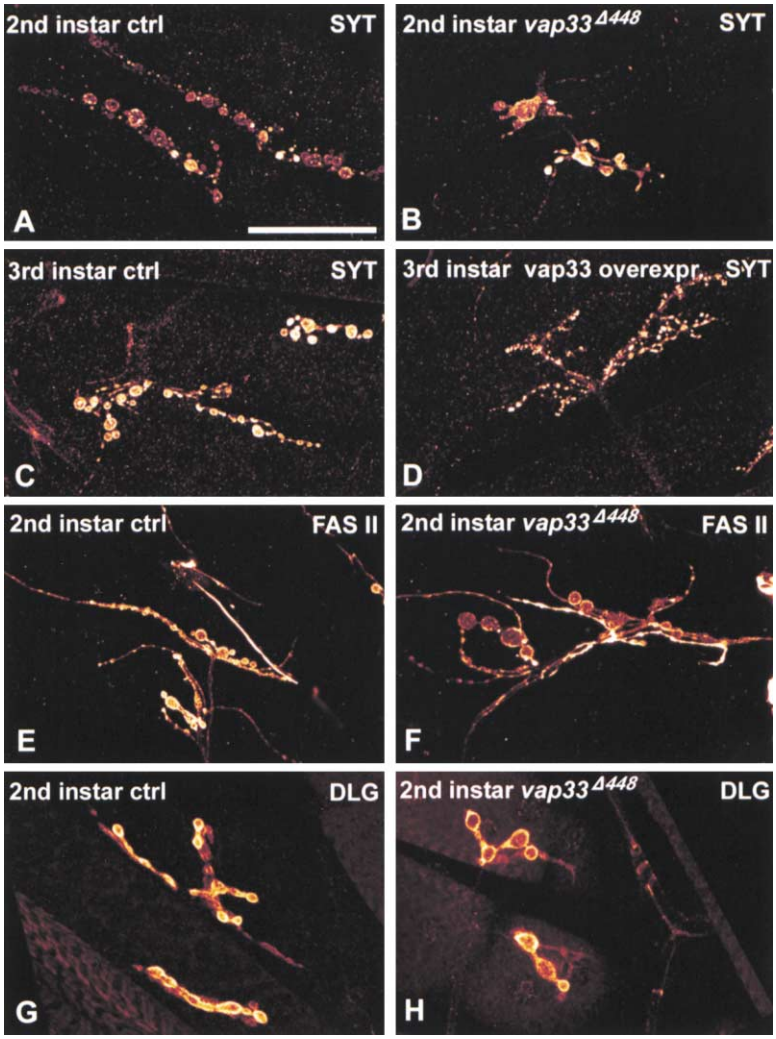

Figure 9. The Localization and Level of Expression of Several Synaptic Markers Are Normal in DVAP-33A Loss-of-Function Mutants and Strains in which DVAP-33A Is Overexpressed

(A and B) *DVAP-33A*$^{\Delta 466}$*/Y* second instar larvae carrying a precise excision of the P element (A) and *DVAP-33A*$^{\Delta 448}$/Y second instar larvae (B) were stained with an antibody specific for Synaptotagmin. (C and D) *UAS-DVAP-33A* third instar larvae (C) and *P{elav-GAL4}; UAS-DVAP-33A* larvae (D) overexpressing DVAP-33A were stained with an antibody anti-Synaptotagmin. (E and F) *DVAP-33A*$^{\Delta 466}$*/Y* second instar larvae resulting from a precise excision of the P element and *DVAP-33A*$^{\Delta 448}$*/Y* second instar larvae were stained with an antibody specific for Fasciclin II (FAS II) and with an antibody directed against Dlg in (G) and (H), respectively. Scale bar: 50 μm.

Stewart, 2000). Assembly of the MSP filaments is directed by a hitherto unidentified integral membrane protein that triggers a site-directed nucleation-elongation reaction (Roberts and Stewart, 2000). The structural similarity between MSPs and VAPs together with its membrane association suggest that DVAP-33A could function as a bridge directing the interaction between the cell membrane and microtubule cytoskeleton during bouton formation. Interestingly, MSP has been shown to function as a bipartite extracellular signaling molecule that promotes oocyte meiotic maturation and smooth muscle contraction in *C. elegans* (Miller et al., 2001). Since DVAP-33A mutants display presynaptic microtubule architecture defects, we favor a cytoskeletal role for DVAP-33A in directing bouton formation. However, our data cannot rule out the possibility that DVAP-33A also plays a signaling function between pre- and postsynaptic sites at the NMJ, especially since our immunolocalization studies suggest that some of the protein may be present at the postsynaptic membrane.

DVAP-33A Is a Membrane Protein that Interacts with Microtubules

Presynaptic membranes consist of several functional regions, each characterized by a distinct molecular composition (Sone et al., 2000). For example, active zones are labeled by anti-DPAK, a *Drosophila* serine/threonine kinase (Sone et al., 2000) and are surrounded by periactive zones, where Dynamin is concentrated and clathrin mediated endocytosis is thought to occur (Estes et al., 1996). Another region of the periactive zone, distinct from the Dynamin domain, contains the proteins controlling synaptic growth and plasticity (Sone et al., 2000). Since immunoreactivity to DVAP-33A overlaps with DLG and complements that of DPAK, we infer that it also marks periactive zones.

Both light and electro-microscopy show that DVAP-33A-specific immunoreactivity is associated with three types of subcellular structures. Most protein is associated with the plasma membrane as well as with the surface of internal vesicular structures. Based on their size and morphological appearance, those vesicles do not seem to be vesicles containing neurotransmitter but rather vesicles required for the transport of synaptic components. Since our data do not support a role for DVAP-33A in axonal transport, we assume that those intracellular vesicular structures represent the form through which DVAP-33A may be transported to its final destination. Ultrastructural and biochemical analysis indicate that the protein is also associated with microtu-

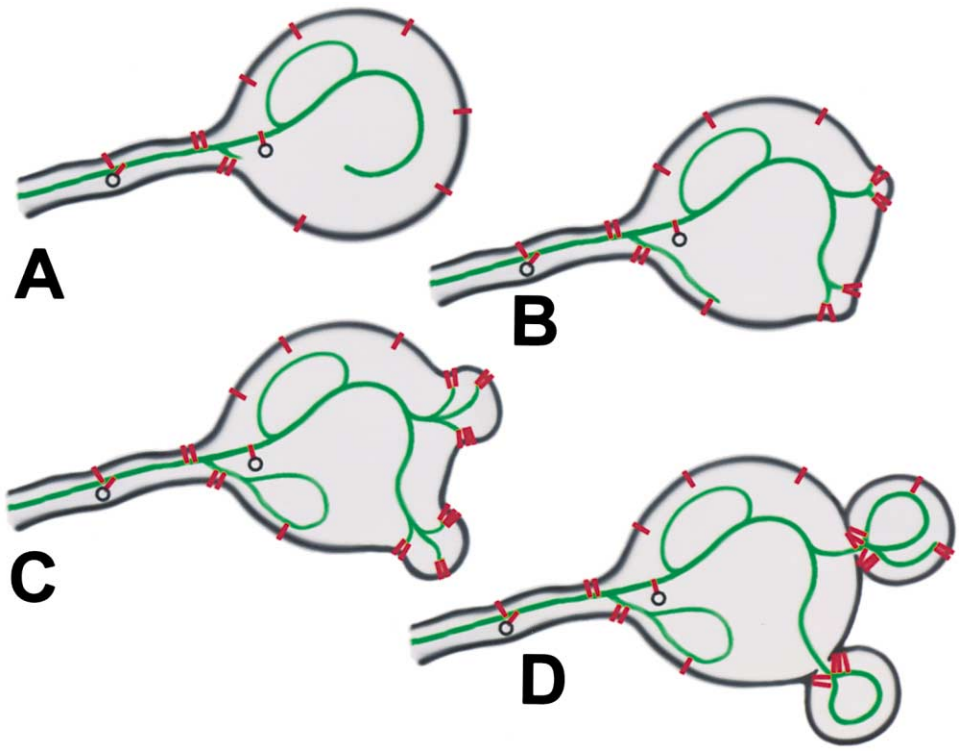

Figure 10. A DVAP-33A-Mediated Interaction between Presynaptic Membrane and Microtubule Cytoskeleton Controls Synaptic Sprouting

(A) Microtubules (green) form bundles inside axons and boutons and loop-like structures in terminal synaptic boutons. (B–D) During budding, the microtubular cytoskeleton splays apart into numerous fibers. At the membrane level, DVAP-33A exhibits particular "hot spots" of concentrated immunoreactivity that are proposed to function as capture sites for microtubule bundles. Interaction between DVAP-33A that is membrane associated and microtubules is proposed to stabilize the microtubules and will initiate the budding of the bouton. Finally, DVAP-33A relocalizes to the base of the newly formed boutons where it promotes the transition of the microtubular array from a fan-like structure to bundles.

bules. Since the primary structure of DVAP-33A predicts a transmembrane domain at its C-terminal, we propose that DVAP-33A associates with microtubules while being anchored to membranes. It is possible that DVAP-33A functions as a bridge between membranes and the microtubule network. It is also important to note that, unlike FUTSCH that decorates microtubules all along their length (Roos et al., 2000), DVAP-33A may overlap with microtubules at specific sites, possibly like CLIP-170, a protein that it is associated with the tip of the microtubules and that functions to stabilize them (Perez et al., 1999). Furthermore, confocal and immuno-electron microscopy show an irregular distribution of the protein at the presumptive sites of new bouton formation. This observation suggests that DVAP-33A can undergo a dynamic relocalization during synapse development. In the emerging bud, the protein seems less abundant at the tip and enriched at both sides of the emerging bud. Subsequently, the protein appears to relocalize at the neck between the two newly forming boutons. The presumptive dynamic localization during bouton formation and the observation that *DVAP-33A* mutants exhibit a reduced number of boutons that are enlarged indicate that *DVAP-33A* plays an important role in bud formation at NMJs.

DVAP-33A Is a Dosage-Dependent Instructive Signal that Regulates Bouton Number or Size

The loss-of-function phenotype associated with *DVAP-33A* in bouton formation indicates that its role may be permissive or instructive. Since presynaptic overexpression of DVAP-33A causes a large increase in number of boutons, it probably plays an instructive role. Moreover, the number of boutons seems to be proportional to the level of DVAP-33A expression, indicating that the latter may directly control synaptic sprouting. A dosage-dependent effect on synaptic growth has previously been ascribed to Fasciclin II, a cell adhesion molecule (Stewart et al., 1996; Schuster et al., 1996b; Davis and Goodman, 1998). In particular, over-sprouting of the synapse is observed in synapses expressing 50% of the wild-type level of FasII (Schuster et al., 1996b). In agreement with these observations, we find that FasII is dramatically downregulated when we overexpress DVAP-33A (G.P. and H.J.B., unpublished data), suggesting that DVAP-33A overexpression creates a molecular environment in the bouton that fosters sprouting. However, loss of DVAP-33A does not affect FasII expression, suggesting that DVAP-33A does not regulate FasII expression.

DVAP-33A Is Required for the Architectural Integrity of Microtubules at the Presynaptic Terminal

The integrity of the microtubular cytoskeleton at the presynaptic terminal is required for boutons to divide and branch. Mutations in *futsch*, which encodes the microtubule-associated protein 1B (MAP1B), cause a phenotype that is similar to the one we observe in *DVAP-33A* mutants: enlarged boutons containing a disrupted

microtubular cytoskeletal network (Roos et al., 2000). We find that in 30% of DVAP-33A boutons, the microtubule network is severely disorganized, whereas in 70% of the boutons, it appears completely disrupted. We therefore propose that DVAP-33A is required for the formation or maintenance of microtubules, and that the subsynaptic architecture of microtubules plays an important role in bouton formation. These observations are also in agreement with the observation that DVAP-33A is associated with microtubules, as is the mouse homolog of VAP-33 (Skehel et al., 2000).

Potential Mechanism of DVAP-33A Function during Bouton Formation at the Synapse

Our ultrastructural analysis indicates that DVAP-33A is associated with both microtubules and intracellular vesicles. This subcellular distribution may imply that DVAP-33A is part of the axonal transport controlling the delivery and/or targeting of synaptic material to the terminals. Our data do not support this hypothesis, however. We propose that a membrane-microtubule interaction, mediated by DVAP-33A, directs and dictates the formation of new synaptic boutons. Zito and colleagues (1999) have shown that new boutons are added at larval NMJs, by a process that structurally resembles budding in yeast. The actual mechanism of cytoskeleton reorganization during bouton budding at NMJs is unknown. Roos et al. (2000) have provided evidence that cytoskeletal rearrangements during bouton sprouting may be similar to the cytoskeletal reorganization occurring during growth cone motility. In both processes, microtubules must rearrange from a bundled array to a more plastic configuration. More particularly, microtubules at the presynaptic terminals are aligned to form a bundle that runs across the boutons. At particular sites, the subsynaptic microtubules are then organized to form a loop, adopting a conformation similar to that acquired by a stalled growth cone (Roos et al., 2000). During formation of a bud, the microtubule loop undergoes a dynamic reorganization during which the looped microtubules splay apart to assume a fan-like structure (Figures 8I and 8K).

We propose that during the transition from a quiescent state to a state of active growth, the microtubules splay apart and explore the inside of the bouton. During this exploratory stage, the microtubules are captured at particular sites in proximity to the membrane. This event, we further propose, then initiates bouton budding. Stabilization of microtubules may be mediated by the interaction between the membrane-associated DVAP-33A and microtubules. Once the bouton starts to bud, DVAP-33A localizes at the base of the bouton where it may stabilize the microtubules by reconverting them into a bundled array of fibers (Figure 10).

The above model may explain many observations. First, lack of DVAP-33A should impair the formation of new boutons (decrease the likelihood of forming new boutons). Second, lack of a protein required to form new boutons should stop growth, leading to enlargement of existing boutons. Third, absence of a membrane localization signal for the microtubules should lead to a disorganized microtubular network. Fourth, increasing the level of DVAP-33A at presynaptic sites may capture more microtubules, thereby increasing the number of the newly formed boutons and branches. Fifth, many proteins associated with the tips of the microtubules are also implicated in microtubules-cortical interactions. These include: EB1, APC, CLASPs, LIS1, and BICD2 (see Dujardin and Vallee, 2002 for a review). Finally, our model is strengthened by the recent finding that Scs2, the yeast homolog of DVAP-33A, is part of a complex controlling nuclear migration during bud formation (Gavin et al., 2002). It has been proposed that this complex functions as a molecular scaffold to search and capture microtubules during bud site selection and elongation (Bloom, 2001; Heil-Chapdelaine et al., 2000; Farkasowsky and Kuntzel, 2001). It is tempting to speculate that a similar molecular mechanism, which controls selection and formation of a new bud in yeast, could control the budding of new boutons at the synapse.

Experimental Procedures

Genetics and Molecular Biology

Basic molecular biology techniques were performed according to Ausubel et al. (1998). Excision mutagenesis of the original P element *P{ry$^{+t7.2}$=IArB}47* and genetic crosses were done following standard protocols.

Drosophila Stocks and Genetics

Excision mutagenesis of the original P element *P{ry$^{+t7.2}$=IArB}47* was performed using the *Sbry^{506}Δ2-3* chromosome (Robertson et al., 1988). All the mutant alleles were balanced over an FM7-GFP chromosome, and non-GFP positive second instar male larvae were selected for the characterization of the loss-of-function phenotype. Mutant and control larvae were staged by following temporal and morphological criteria as described in Biology of *Drosophila* (Demerec, 1950). To test whether lethality was associated with a mutation in *DVAP-33A*, we crossed *DVAP-33A^{Δ20}/FM7 or DVAP-33A^{Δ448}/FM7* females to *y w/Y; P{CaSpeR-hs-DVAP-33A}/P{CaSpeR-hs-DVAP-33A}* males. The flies were maintained in a cycling incubator and received a 1 hr heat shock (37°C) every 7 hr. A significant number of *DVAP-33A^{Δ20}/Y; P{CaSpeR-hs-DVAP-33A}/+* and *DVAP-33A^{Δ448}/Y; P{CaSpeR-hs-DVAP-33A}/+* adult flies were recovered, suggesting that the lethality was due specifically to mutations in *DVAP-33A*. We also crossed *y w/Y; C164-GAL4/C164-GAL4* males to either *DVAP-33A^{Δ20}/FM7; +/+; UAS-DVAP-33A/UAS-DVAP-33A* or *DVAP-33A^{Δ448}/FM7, +/+; UAS-DVAP-33A/UAS-DVAP-33A* females. *DVAP-33A^{Δ20}/Y; C164-GAL4/+; UAS-DVAP-33A/+* and *DVAP-33A^{Δ448}/Y; C164-GAL4/+; UAS-DVAP-33A/+* were identified as Bar+, non FM7 males, again suggesting that the lethality is linked to mutations in the *DVAP-33A* locus. To test dosage dependence, females *DVAP-33A^{Δ448}/FM7; +/+; UAS-DVAP-33A/UAS-DVAP-33A* were crossed to *+/Y; C164-GAL4/C164-GAL4* males. Embryos were collected for 8 hr and then transferred to either 30°C or 18°C. *DVAP-33A^{Δ448}/Y; C164-GAL4/+; UAS-DVAP-33A/+* third instar larval males were identified as y+ larvae lacking the FM7 balancer chromosome. To characterize the overexpression phenotype, *elaV-GAL4/elaV-GAL4* females were crossed to *y w/Y; +/+; UAS-VAP-33A/UAS-VAP-33A*. Embryos were collected for 8 hr and transferred to a water bath at 30°C. Third instar larval NMJs were examined for a mutant phenotype. The same overexpression phenotype was observed by using *P{Gal4w^{+}}C164*, another motor neuron-specific GAL4 driver.

Immunocytochemistry

The full-length DVAP-33A cDNA was cloned into pET-28a(+) expression vector (Novagen) to make an His-tag fusion protein. A guinea pig polyclonal antibody was produced against this protein and used at a concentration of 1:10,000 on Western blot analyses and at 1:200 for NMJ immunocytochemistry. Dissected larval NMJs were stained with several antibodies as described in Bellen and Budnik (2000).

Dissected larval NMJs were fixed in Bouin's fixative (15:5:1 mixture of saturated picric acid, 37% formaldehyde and glacial acetic

acid) for 10 min, washed extensively in PBT (PBS +0,1% TritonX-100), blocked in 10% normal goat serum in PBT for 2 hr, and finally incubated with the primary antibody overnight at 4°C. Rabbit anti-HRP antibody (Jackson ImmunoResearch Labs) was used at 1:200; mouse anti-DLG antibody was used at a 1:200; monoclonal antibody 22C10 at 1:500; monoclonal anti-α-tubulin antibody (Sigma) at 1:500; rabbit anti-DPAK antibody at 1:500. Fluorescent secondary antibodies were used at 1:400. For anti-HRP staining, a goat biotinylated anti-rabbit secondary antibody was used (Vector laboratories). Signal detection was carried out with a VectaStain ABC-HRP kit (Vector laboratories). To quantify the mutant phenotype, at least 20 different synapses per genotype were counted.

Immuno-Electron Microscopy

Pre-embedding immunolabeling was performed on the heads of four *Drosophila* adults and more than six filleted third instar larvae. These were dissected in 0.01 M phosphate buffer (PB, pH 7.4) containing 4% paraformaldehyde, 1% glutaraldehyde, and 0.01% picric acid and fixed for 30 min on ice; washed in PB (2 × 10 min); the fly heads embedded in 7% agarose and sliced at 80 μm by a Vibratome. Slices or whole-mounted larvae were incubated in 1% glycine/PB (1 hr); washed in PB (3 × 10 min); permeabilized with 0.1% Saponin (Sigma) in blocking medium (BM) comprising PB with 1% bovine serum albumin (Sigma), 10% normal goat serum (GIBCO) (1 hr at 4°C); incubated in primary polyclonal anti-DVAP33A antiserum (see above) at 1:100 in BM containing 0.01% Saponin for 48 hr at 4°C; washed in PB (5 × 10 min); and kept overnight in a large volume of PB at 4°C. After renewed permeabilization in BM, preparations were incubated with anti-guinea pig secondary antibody coupled to 1.4 nm gold particles (Nanoprobes) (1:100; 48 hr at 4°C). After thorough washing in PB for 48 hr, gold particles were silver intensified and specimens osmicated and embedded according to Skehel et al. (2000). Ultrathin sections (60 nm) were collected on Pioloform-coated single-slot copper grids and contrasted with uranyl acetate and Reynold's lead citrate.

Three-Dimensional Visualization and Quantification of Confocal Image Data

Most confocal data were acquired as image stacks of separate channels with a Zeiss LSM 510 microscope and combined and visualized with Amira 2.3 (Indeed GmbH, Berlin, Germany). Final pictures were obtained as maximum intensity projections or emission/absorption volume renderings from different viewpoints with cutaways of parts of the volume. For quantification of bouton size, high-resolution scans of single bouton scans were threshold-segmented, triangularized surfaces generated using the generalized marching cubes algorithm, and the total surface areas determined. For the visualization of microtubular networks, high-resolution confocal scans with voxel sizes of 140 × 140 × 200 nm were deconvoluted using a 3D blind deconvolution algorithm (Hiesinger et al., 2001). Surface models were generated from hand-segmented structures. Figures were assembled and labeled in Adobe Photoshop.

Microtubule Pulldown Assay

Determination of the ability of DVAP-33A to cosediment with exogenously added microtubules was performed according to the manufacturer's protocol (Cytoskeleton, Denver) with some modifications according to Lantz and Miller (1998). Whole head extracts were made in our extraction buffer containing 5 mM Hepes (pH 7.4) and NaCl 100 mM in the presence of a cocktail of protease's inhibitors (Roche Diagnostics). The extract was clarified by centrifugation at 5000 × g for 20 min at 4°C. The supernatant was incubated with 1% Triton X-100 at 4°C under constant agitation for 1 hr. The extracts were centrifuged at 50,000 rpm (rotor TL100) for 20 min at 4°C. The protein content of the high speed supernatant was determined according to the Bradford assay and equivalent amounts of proteins were incubated with in vitro polymerized microtubules or without microtubules, following the protocol proposed by the manufacturer. Both reactions were stratified on a 20% sucrose cushion and centrifuged at 37,000 rpm (rotor TL100) for 30 min. The resulting supernatants and pellets were analyzed by SDS-PAGE and Western analysis.

Acknowledgments

We thank L. Zipursky, N. Harden, C. Goodman, P. Bryant, and V. Budnik for antibodies. We also thank D. Greenstein, V. Budnik, and A. Fayyazuddin for critical reading. We thank J. Kunz for stimulating discussions and Y. Zhou for technical assistance. G.P. is supported by HHMI, P.R.H. by EMBO, R.F.F. by the Killam Trust of Dalhousie University, and I.A.M. by NIH grant EY-03592 and by the Killam Trust of Dalhousie University. H.J.B. is an Investigator of the HHMI.

Received: December 11, 2001
Revised: April 29, 2002

References

Atwood, H.L., Govind, C.K., and Wu, C.F. (1993). Differential ultrastructure of synaptic terminals on ventral longitudinal abdominal muscles in *Drosophila* larvae. J. Neurobiol. *24*, 1008–1024.

Ausubel, F.M., Brent, R., Kingston, R.E., Moore, D.D., Seidman, J.G., Smith, J.A., and Struhl, K. (1998). Current protocols in molecular biology. John Wiley and Sons, Inc.

Bellen, H.J., and Budnik, V. (2000). The neuromuscular junction. In Drosophila, A Laboratory Manual. M. Ashburner, S. Hawley, and B. Sullivan, eds. (Cold Spring Harbor, NY: Cold Spring Harbor Laboratory).

Bellen, H.J., O'Kane, C.J., Wilson, C., Grossniklaus, U., Pearson, R.K., and Gehring, W.J. (1989). P-element-mediated enhancer detection: a versatile method to study development in *Drosophila*. Genes Dev. *3*, 1288–1300.

Bilder, D., Li, M., and Perrimon, N. (2000). Cooperative regulation of cell polarity and growth by Drosophila tumor suppressors. Science *289*, 113–116.

Bloom, K. (2001). Nuclear migration: cortical anchors for cytoplasmic dynein. Curr. Biol. *11*, 326–329.

Brand, A.H., and Perrimon, N. (1993). Targeted gene expression as a means of altering cell fates and generating dominant phenotypes. Development *118*, 401–415.

Budnik, V., Zhong, Y., and Wu, C.-F. (1990). Morphological plasticity of motor axons in *Drosophila* mutants with altered excitability. J. Neurosci. *10*, 3754–3768.

Budnik, V., and Gramates, L.S., eds. (1999). Neuromuscular Junctions in Drosophila (London: Academic Press).

Davis, G.W., and Goodman, C.S. (1998). Synapse-specific control of synaptic efficacy at the terminals of a single neuron. Nature *392*, 82–86.

Davis, G.W., Schuster, C.M., and Goodman, C.S. (1996). Genetic dissection of structural and functional components of synaptic plasticity. III. CREB is necessary for presynaptic functional plasticity. Neuron *17*, 669–679.

Demerec, M. (1950). Biology of Drosophila (New York: John Wiley & Sons, Inc).

Dujardin, D.L., and Vallee, R.B. (2002). Dynein at the cortex. Curr. Opin. Cell Biol. *14*, 44–49.

Engert, F., and Bonhoeffer, T. (1999). Dendritic spine changes associated with hippocampal long-term synaptic plasticity. Nature *399*, 19–21.

Estes, P.S., Roos, J., van der Bliek, A., Kelly, R.B., Krishnan, K.S., and Ramaswami, M. (1996). Traffic of dynamin within individual Drosophila synaptic boutons relative to compartment-specific markers. J. Neurosci. *16*, 5443–5456.

Farkasowsky, M., and Kuntzel, H. (2001). Cortical Num1p interacts with the dynein intermediate chain Pac11p and cytoplasmic microtubules in budding yeast. J. Cell Biol. *152*, 251–262.

Galaud, J.P., Laval, V., Carriere, M., Barre, A., Canut, H., Rouge, P., and Pont-Lezica, R. (1997). Osmotic stress activated expression of an Arabidopsis plasma membrane-associated protein: sequence and predicted secondary structure. Biochem. Biophys. Acta *1341*, 79–86.

Gavin, A.C., Bosche, M., Krause, R., Grandi, P., Marzioch, M., Bauer,

A., Schultz, J., Rick, J.M., Michon, A.M., Cruciat, C.M., et al. (2002). Functional organization of the yeast proteome by systematic analysis of protein complexes. Nature *415*, 123–124.

Gindhart, J.G., Desai, C.J., Beushausen, S., Zinn, K., and Goldstein, L.S. (1998). Kinesin light chains are essential for axonal transport in Drosophila. J. Cell Biol. *141*, 443–454.

Goode, B.L., and Feinstein, S.C. (1994). Identification of a novel microtubule binding and assembly domain in the developmentally regulated inter-repeat region of tau. J. Cell Biol. *124*, 769–782.

Gorczyca, M., Augart, C., and Budnik, V. (1993). Insulin-like receptor and insulin-like peptide are localized at neuromuscular junctions in Drosophila. J. Neurosci. *13*, 3692–3704.

Greenspan, R.J. (1997). Fly Pushing: The Theory and Practice of *Drosophila* Genetics. (Cold Spring Harbor, NY: Cold Spring Harbor Laboratory Press).

Gunawardena, S., and Goldstein, L.S. (2001). Disruption of axonal transport and neuronal viability by amyloid precursor protein mutations in *Drosophila*. Neuron *32*, 389–401.

Heil-Chapdelaine, R.A., Oberle, J.R., and Cooper, J.A. (2000). The cortical protein Num1p is essential for dynein-dependent interactions of microtubules with the cortex. J. Cell Biol. *151*, 1337–1344.

Hiesinger, P.R., Scholz, M., Meinertzhagen, I.A., Fischbach, K.F., and Obermayer, K. (2001). Visualization of synaptic markers in the optic neuropils of *Drosophila* using a new constrained deconvolution method. J. Comp. Neurol. *429*, 277–288.

Hummel, T., Krukkert, K., Roos, J., Davis, G., and Klambt, C. (2000). *Drosophila* Futsch/22C10 is a MAP1B-like protein required for dendritic and axonal development. Neuron *26*, 357–370.

Italiano, J.E., Jr., Roberts, T.M., Stewart, M., and Fontana, C.A. (1996). Reconstitution in vitro of the motile apparatus from the amoeboid sperm of Ascaris shows that filament assembly and bundling move membranes. Cell *84*, 105–114.

Jan, L.Y., and Jan, Y.N. (1982). Antibodies to horseradish peroxidase as specific neuronal markers in Drosophila and in grasshopper embryos. Proc. Natl. Acad. Sci. USA *79*, 2700–2704.

Johansen, J., Halpern, M.E., Johansen, K.M., and Keshishian, H. (1989). Stereotypic morphology of glutamatergic synapses on identified muscle cells of Drosophila larvae. J. Neurosci. *9*, 710–725.

Kagiwada, S., Hosaka, K., Murata, M., Nikawa, J., and Takatsuki, A. (1998). The Saccharomyces cerevisiae SCS2 gene product, a homolog of a synaptobrevin-associated protein, is an integral membrane protein of the endoplasmic reticulum and is required for inositol metabolism. J. Bacteriol. *180*, 1700–1708.

Lahey, T., Gorczyca, M., Jia, X.X., and Budnik, V. (1994). The *Drosophila* tumor suppressor gene dlg is required for normal synaptic bouton structure. Neuron *13*, 823–835.

Lantz, V.A., and Miller, K.J. (1998). A class VI unconventional myosin is associated with a homologue of a microtubule-binding protein, cytoplasmic linker protein-170, in neurons and at the posterior pole of *Drosophila* embryos. J. Cell Biol. *140*, 897–910.

Lapierre, L.A., Tuma, P.L., Navarre, J., Goldenring, J.R., and Anderson, J.M. (1999). VAP-33 localizes to both an intracellular vesicle population and with occludin at the tight junction. J. Cell Sci. *112*, 3723–3732.

Laurent, F., Labesse, G., and de Wit, P. (2000). Molecular cloning and partial characterization of a plant VAP33 homologue with a major sperm protein domain. Biochem. Biophys. Res. Commun. *270*, 286–292.

Lin, D.M., and Goodman, C.S. (1994). Ectopic and increased expression of fasciclin II alters motoneuron growth cone guidance. Neuron *13*, 507–523.

Lloyd, T.E., Verstreken, P., Ostrin, E.J., Phillippi, A., Lichtarge, O., and Bellen, H.J. (2000). A genome-wide search for synaptic vesicle cycle proteins in Drosophila. Neuron *26*, 45–50.

Maletic-Savatic, M., Malinow, R., and Svoboda, K. (1999). Rapid dendritic morphogenesis in CA1 hippocampal dendrites induced by synaptic activity. Science, 1923–1927.

Martin, M., Iyadurai, S.J., Gassman, A., Gindhart, J.G., Hays, T.S., and Saxton, W.M. (1999). Cytoplasmic dynein, the dynactin complex, and kinesin are interdependent and essential for fast axonal transport. Mol. Biol. Cell *10*, 3717–3728.

Miller, M.A., Nguyen, V.Q., Lee, M.H., Kosinski, M., Schedl, T., Caprioli, R.M., and Greenstein, D. (2001). A sperm cytoskeletal protein that signals oocyte meiotic maturation and ovulation. Science *291*, 2144–2147.

Nikawa, J., Murakami, A., Esumi, E., and Hosaka, K. (1995). Cloning and sequence of the SCS2 gene, which can suppress the defect of INO1 expression in an inositol auxotrophic mutant of Saccharomyces cerevisiae. J. Biochem. (Tokyo) *118*, 39–45.

Ohshiro, T., Yagami, T., Zhang, C., and Matsuzaki, F. (2000). Role of cortical tumour-supressor proteins in asymmetric division of Drosophila neuroblast. Nature *408*, 593–596.

Peng, C.Y., Manning, L., Albertson, R., and Doe, C.Q. (2000). The tumour-suppressor genes lgl and dlg regulate basal protein targeting in Drosophila neuroblasts. Nature *408*, 596–600.

Perez, F., Diamantopoulos, G.S., Stalder, R., and Kreis, T.E. (1999). CLIP-170 highlights growing microtubule ends in vivo. Cell *96*, 517–527.

Roberts, T.M., and Stewart, M. (2000). Acting like actin. The dynamics of the nematode major sperm protein (msp) cytoskeleton indicate a push-pull mechanism for amoeboid cell motility. J. Cell Biol. *149*, 7–12.

Robertson, H.M., Preston, C.R., Phillis, R.W., Johnson-Schlitz, D.M., Benz, W.K., and Engels, W.R. (1988). A stable genomic source of P element transposase in Drosophila melanogaster. Genetics *118*, 461–470.

Roos, J., Hummel, T., Ng, N., Klambt, C., and Davis, G.W. (2000). *Drosophila* Futsch regulates synaptic microtubule organization and is necessary for synaptic growth. Neuron *26*, 371–382.

Sanes, J.R., and Lichtman, J.W. (1999). Development of the vertebrate neuromuscular junction. Annu. Rev. Neurosci. *22*, 389–442.

Schuster, C.M., Davis, G.W., Fetter, R.D., and Goodman, C.S. (1996a). Genetic dissection of structural and functional components of synaptic plasticity. I. Fasciclin II controls synaptic stabilization and growth. Neuron *17*, 641–654.

Schuster, C.M., Davis, G.W., Fetter, R.D., and Goodman, C.S. (1996b). Genetic dissection of structural and functional components of synaptic plasticity. II. Fasciclin II controls presynaptic structural plasticity. Neuron *17*, 655–667.

Skehel, P.A., Martin, K.C., Kandel, E.R., and Bartsch, D. (1995). A VAMP-binding protein from Aplysia required for neurotransmitter release. Science *236*, 1580–1583.

Skehel, P.A., Fabian-Fine, R., and Kandel, E.R. (2000). Mouse VAP33 is associated with the endoplasmic reticulum and microtubules. Proc. Natl. Acad. Sci. USA *97*, 1101–1106.

Sone, M., Hoshino, M., Suzuki, E., Kuroda, S., Kaibuchi, K., Nakagoshi, H., Saigo, K., Nabeshima, Y., and Hama, C. (1997). Still life, a protein in synaptic terminals of *Drosophila* homologous to GDP-GTP exchangers. Science *275*, 543–547.

Sone, M., Suzuki, E., Hoshino, M., Hou, D., Kuromi, H., Fukata, M., Kuroda, S., Kaibuchi, K., Nabeshima, Y., and Hama, C. (2000). Synaptic development is controlled in the periactive zones of *Drosophila* synapses. Development *127*, 4157–4168.

Soussan, L., Burakov, D., Daniels, M.P., Toister-Achituv, M., Porat, A., Yarden, Y., and Elazar, Z. (1999). ERG30, a VAP-33-related protein, functions in protein transport mediated by COPI vesicles. J. Cell Biol. *146*, 301–311.

Stewart, B.A., Schuster, C.M., Goodman, C.S., and Atwood, H.L. (1996). Homeostasis of synaptic transmission in Drosophila with genetically altered nerve terminal morphology. J. Neurosci. *16*, 3877–3886.

Toni, N., Buchs, P.A., Nikonenko, I., Bron, C.R., and Muller, D. (1999). LTP promotes formation of multiple spine synapses between a single axon terminal and a dendrite. Nature *402*, 421–425.

Torroja, L., Packard, M., Gorczyca, M., White, K., and Budnik, V. (1999). The *Drosophila* beta-amyloid precursor protein homolog promotes synapse differentiation at the neuromuscular junction. J. Neurosci. *19*, 7793–7803.

Zhong, Y., Budnik, V., and Wu, C.-F. (1992). Synaptic plasticity in *Drosophila* memory and hyperexcitable mutants—role of cAMP cascade. J. Neurosci. *12*, 644–651.

Zito, K., Parnas, D., Fetter, R.D., Isacoff, E.Y., and Goodman, C.S. (1999). Watching a synapse grow: noninvasive confocal imaging of synaptic growth in *Drosophila*. Neuron *22*, 719–729.